

## **Dimorphs of 1:1 cocrystal of ethenzamide and saccharin: solid-state grinding methods result in metastable polymorph**

Srinivasulu Aitipamula,<sup>\*,a</sup> Pui Shan Chow,<sup>a</sup> and Reginald B.H. Tan<sup>\*,a,b</sup>

<sup>a</sup>*Institute of Chemical and Engineering Sciences, A\*STAR (Agency for Science, Technology and Research), 1, Pesek Road, Jurong Island, Singapore, 627833.*

<sup>b</sup>*Department of Chemical & Biomolecular Engineering, National University of Singapore, 4 Engineering Drive 4, Singapore 117576.*

Email: srinivasulu\_aitipamula@ices.a-star.edu.sg

### **Electronic Supplementary Information**

#### **Contents**

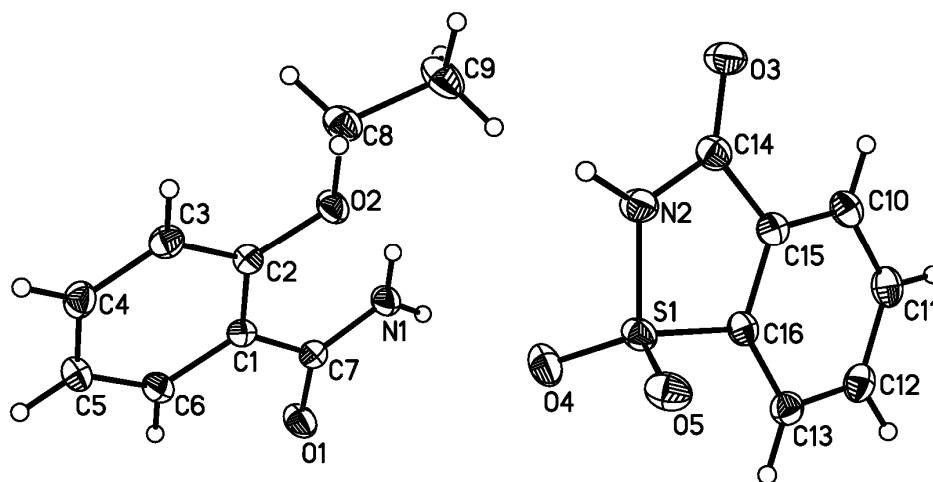
**Figs. S1-S2 - ORTEP diagrams**

**Figs. S3-S5 - Additional Figures for crystal packing of Form II**

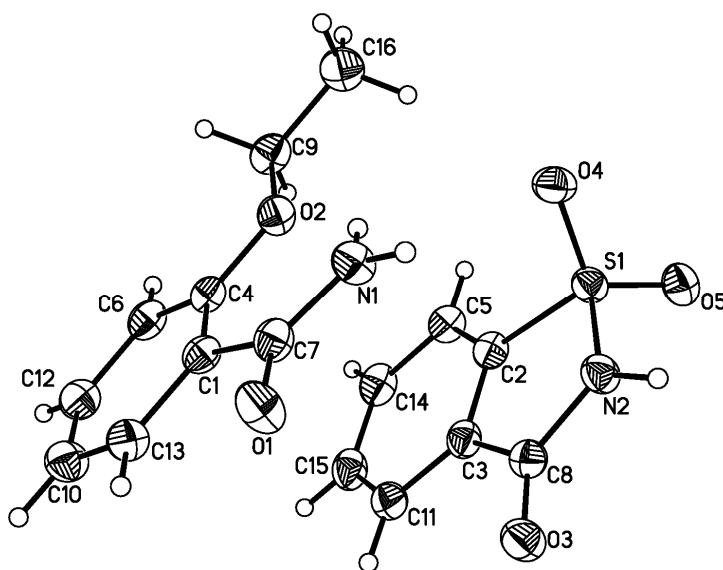
**Figs. S6-S10 - Comparison of PXRD patterns of various grinding experiments.**

**Fig. S11-12- Comparison of PXRD patterns of sublimation products**

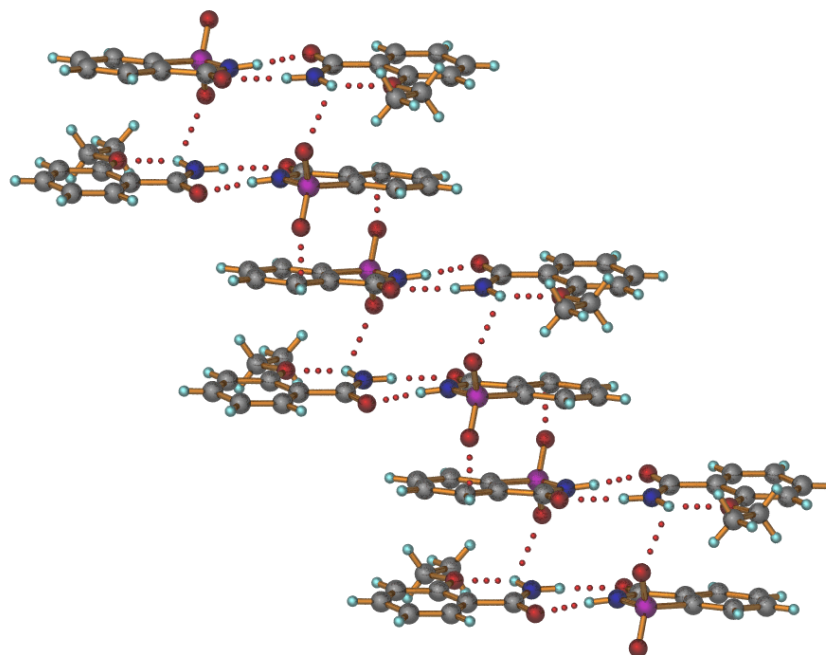
**Fig. S13 - DSCs of Forms I and II**



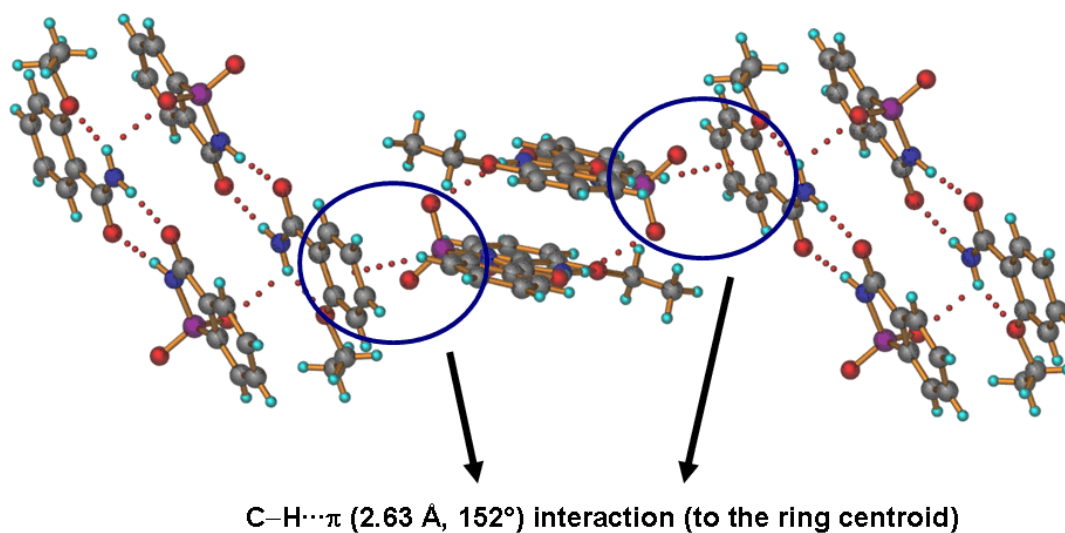
**Fig. S1** ORTEP diagram for Form I showing the atom numbering. Thermal ellipsoids were drawn at 50 % probability.



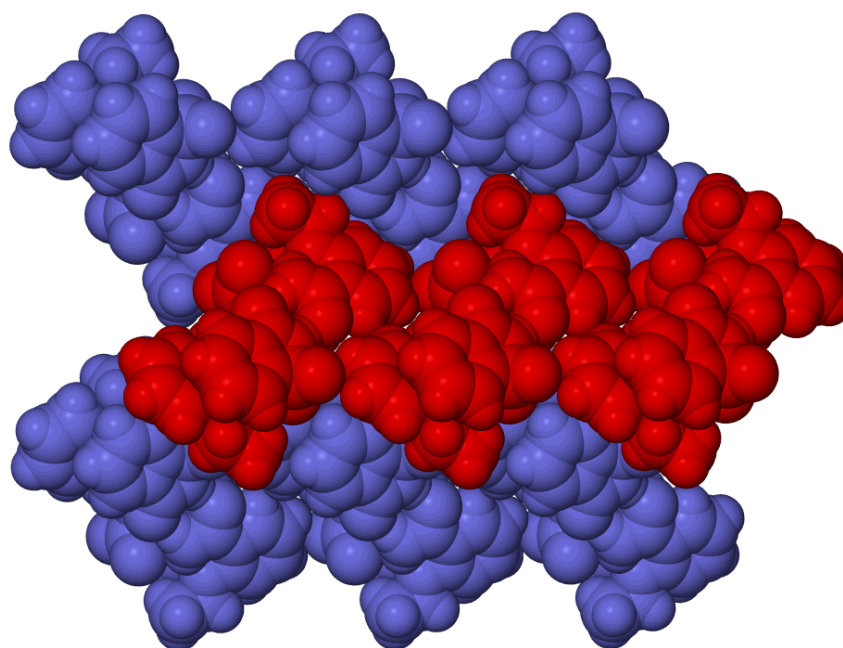
**Fig. S2** ORTEP diagram for Form II showing the atom numbering. Thermal ellipsoids were drawn at 50 % probability.



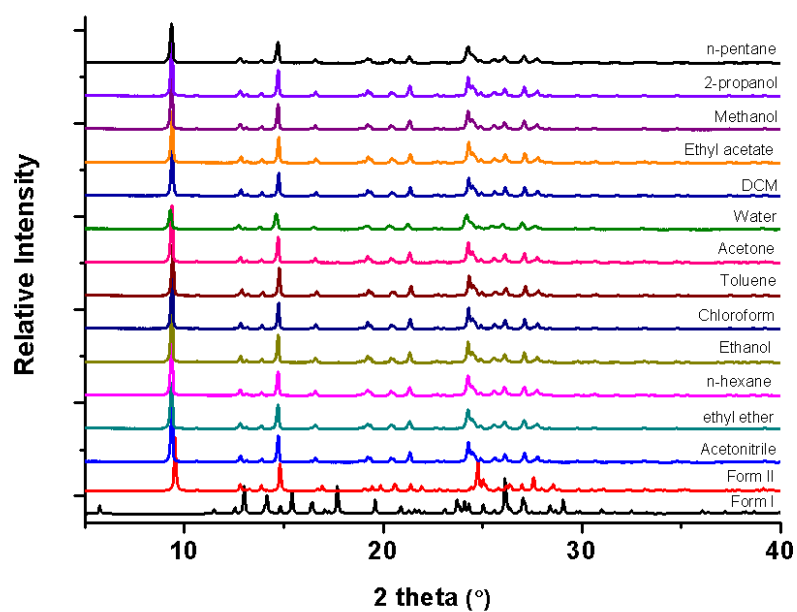
**Fig. S3** Part of the crystal structure of Form II, showing the arrangement of tetrameric motifs held together by a C–H...O (2.41–2.72 Å, 119–152°) interactions with an offset.



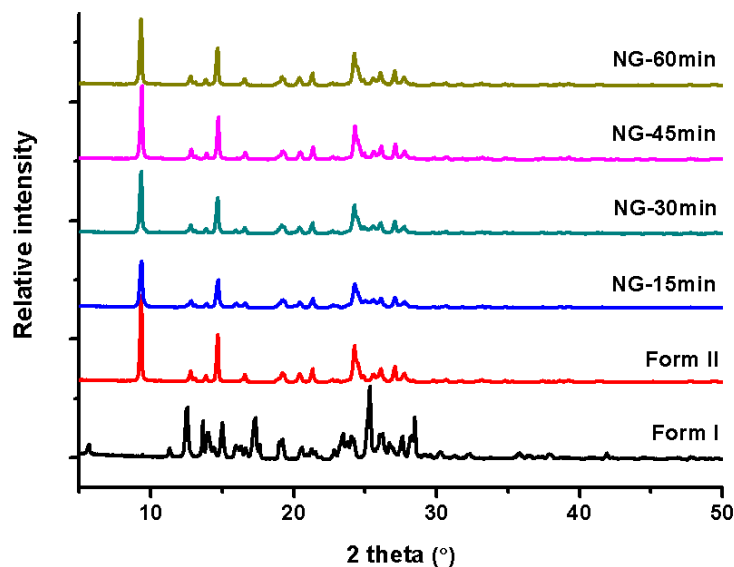
**Fig. S4** C–H... $\pi$  interactions between the tetrameric motifs in the crystal structure of Form II.



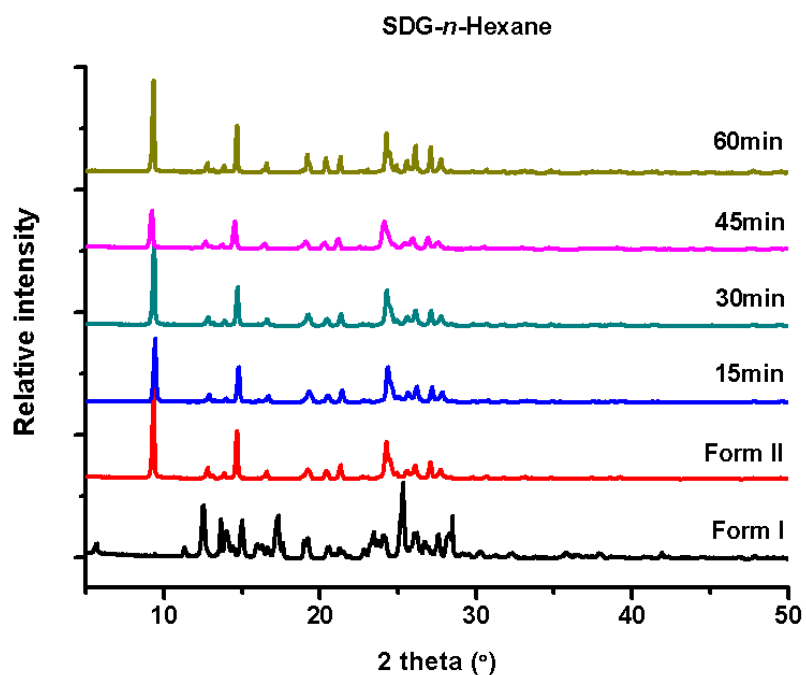
**Fig. S5** Herringbone arrangement of tetrameric motifs in the crystal structure of Form II.



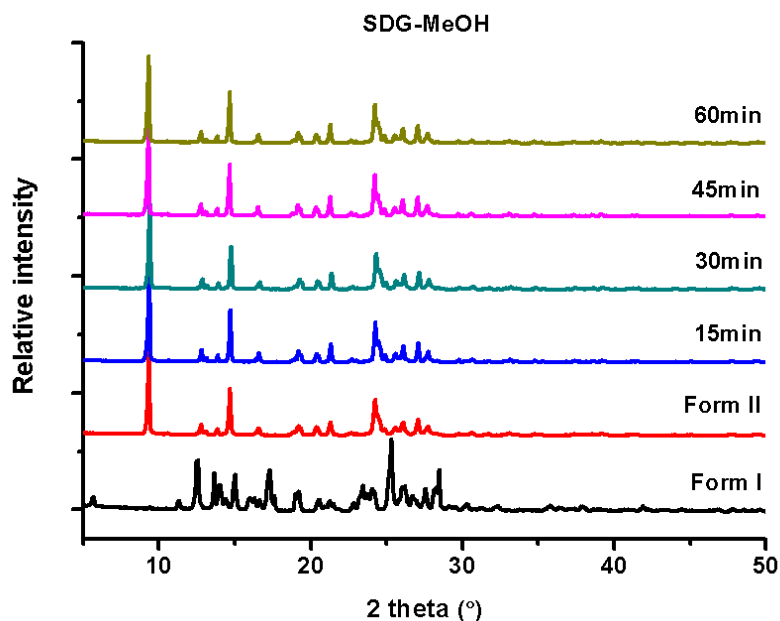
**Fig. S6** Comparison of the PXRD patterns of the powder materials obtained from the SDG experiments. Notice that all the patterns match perfectly with metastable Form II.



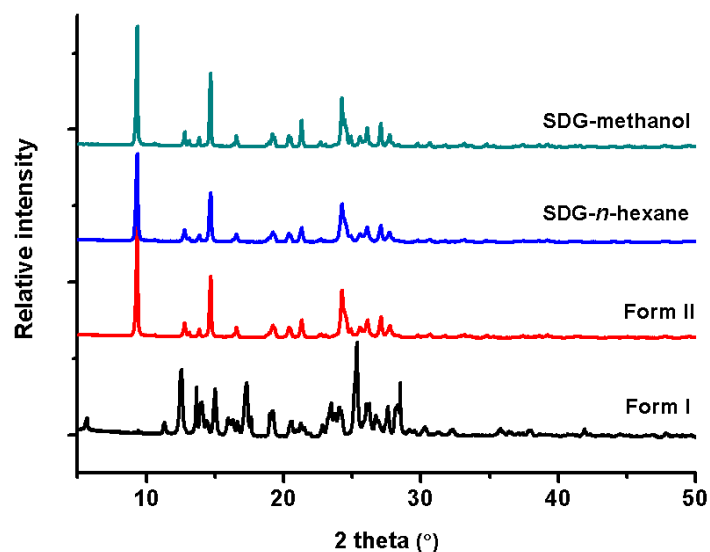
**Fig. S7** Comparison of the PXRD patterns of the powder materials obtained from the NG experiments with varying grinding time. Notice that all the patterns match perfectly with Form II.



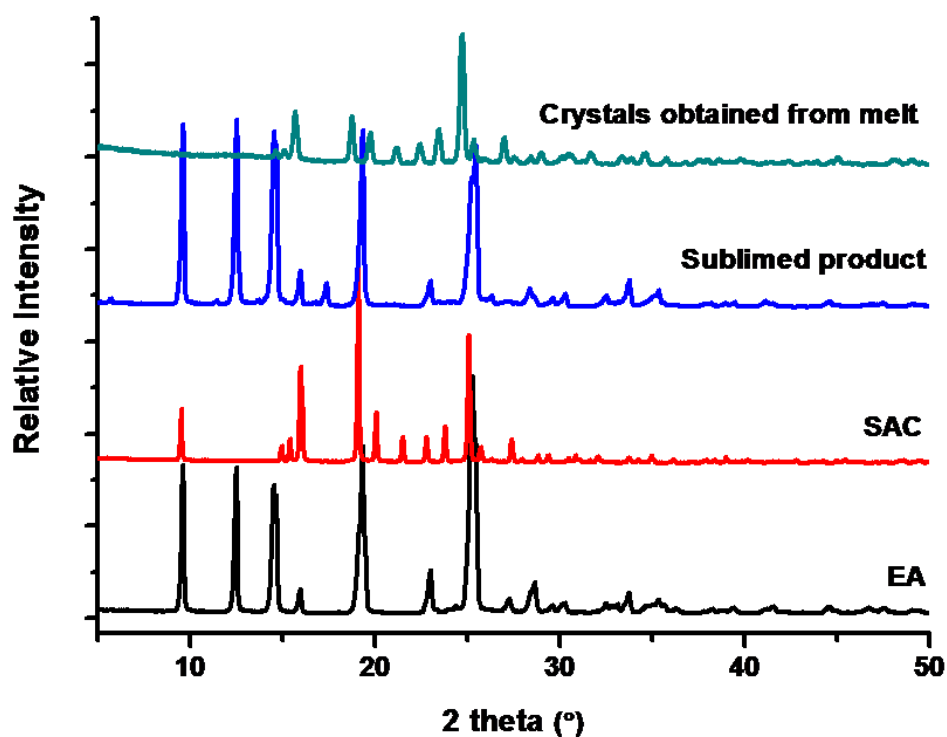
**Fig. S8** Comparison of the PXRD patterns of the powder materials obtained from the SDG experiments with a nonpolar solvent (*n*-hexane) with varying grinding time. Notice that all the patterns match perfectly with Form II.



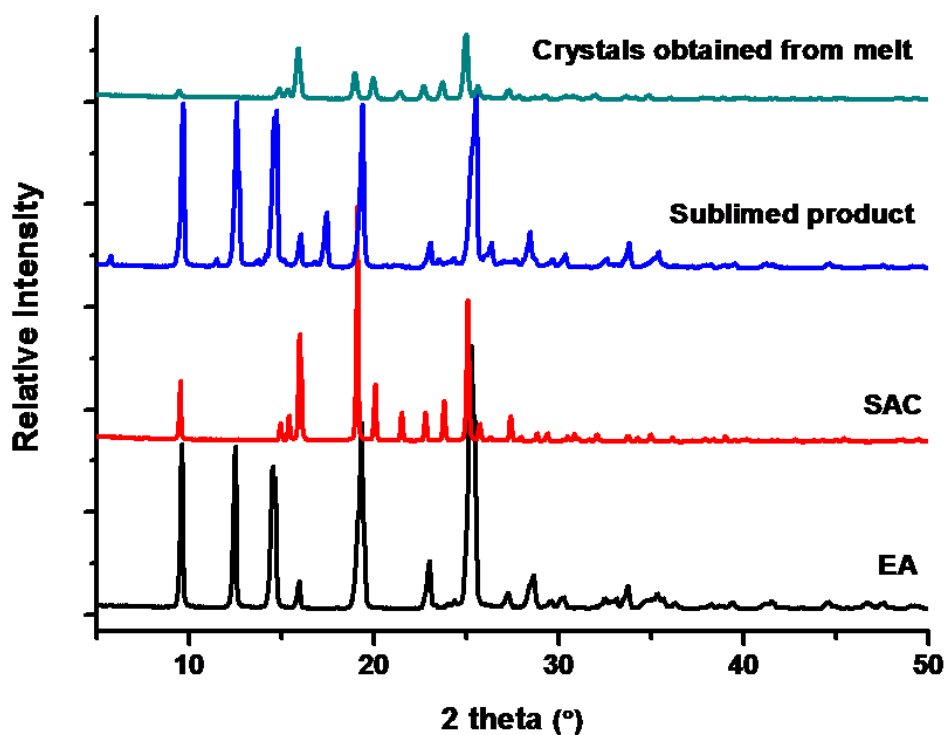
**Fig. S9** Comparison of the PXRD patterns of the powder materials obtained from the SDG experiments with a polar solvent (methanol) with varying grinding time. Notice that all the patterns match perfectly with Form II.



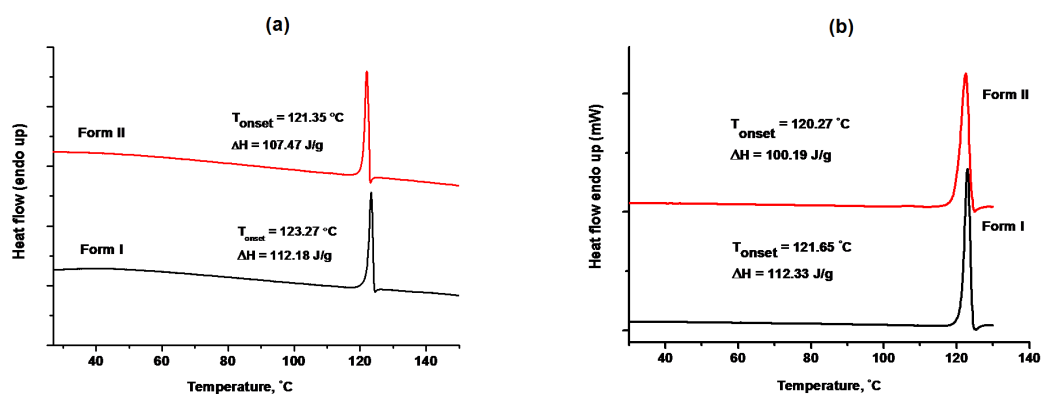
**Fig. S10** Comparison of the PXRD patterns of the powder materials obtained from further SDG experiments on Form II. Notice that both the patterns match perfectly with Form II.



**Fig. S11** Comparison of the PXRD patterns of the products obtained from sublimation experiment on Form I. Note that sublimed product matches with EA and the crystals obtained from the melt matches with SAC.



**Fig. S12** Comparison of the PXRD patterns of the products obtained from sublimation experiment on Form II. Note that sublimed product matches with EA and the crystals obtained from the melt matches with SAC.





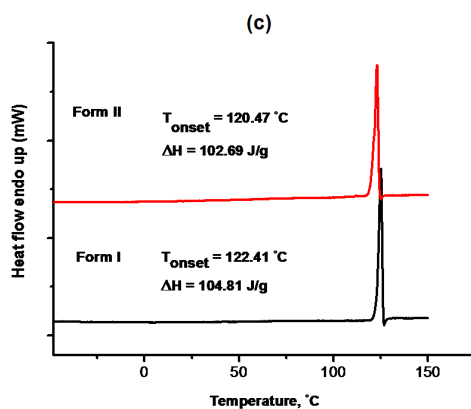


**Fig. S13** DSC curves of Forms I and II recorded on the samples obtained from different crystallization (Form I) and grinding experiments (Form II). Note that heat of fusion for the melting of Form I is higher when compared to the Form II in all the DSC experiments.